1-1-2007

13.5 nm EUV generation from tin-doped droplets using a fiber laser

Simi A. George
University of Central Florida

Kai-Chung Hou

Kazutoshi Takenoshita
University of Central Florida

Almantas Galvanauskas

Martin C. Richardson
University of Central Florida

13.5 nm EUV generation from tin-doped droplets using a fiber laser

Simi A. George[1,2], **Kai-Chung Hou**[3], **Kazutoshi Takenoshita**[1], **Almantas Galvanauskas**[3] **and Martin C. Richardson**[1]

1. Laser Plasma Laboratory, College of Optics & Photonics: CREOL & FPCE, University of Central Florida, Orlando, Florida 32816

2. Department of Physics, University of Central Florida, Orlando, Florida 32816

3. Center for Ultrafast Optical Sciences, University of Michigan, 2200 Bonisteel Blvd, Ann Arbor, Michigan 48109

sgeorge@creol.ucf.edu

Abstract: A comprehensive study of the spectral and Mo-Si mirror in-band EUV emission from tin-doped droplet laser plasma targets irradiated with a single 1064 nm beam from an Yb:doped fiber laser is reported. With pre-pulse enhancement, in-band conversion efficiency of approximately 2.1% is measured for laser irradiance intensities near 8×10^{10} W/cm^2. This is the first study to be reported that uses a high-power, high repetition rate fiber laser with the high repetition rate droplet targets where EUV generation from plasmas is measured.

OCIS codes: (300.0300) Spectroscopy; (340.0340) X-ray Optics; (000.0000) General.

References and links

1. C. W. Gwyn, R. Stulen, D. Sweeney, and D. Attwood, "Extreme ultraviolet lithography," J. Vac. Sci. Technol. B **16**, 3142–3149 (1998).
2. S. Bajt, J. B. Alameda, T. W. Barbee, Jr., W. M. Clift, J.A. Folta, B.B. Kaufmann, and E. A. Spiller, "Improved reflectance and stability of Mo/Si multilayers," Proc. SPIE **(**4506), 65–75 (2001).
3. V. Bakshi, *EUV Sources for Lithography*(SPIE Press, Washington, 2005)
4. A. Miyake and H. Kanazawa and V. Banine and K. Suzuki, "Joint Requirements," Presentation at EUV Workshop, October 19, 2006. Proceedings available at www.sematech.org
5. D. T. Attwood, *Soft x-rays and extreme ultraviolet radiation: principles and applications* (Cambridge University Press, Berkeley, 2000).
6. S. Ellwi, "High Power lasers for EUV sources." Presentation at EUV Source Workshop, May 6, 2007, Baltimore MA.
7. D. Brandt, "LPP EUV Source Development for HVM," Presented at EUVL symposium, Barcelona, Spain, Oct. 17 2006.
8. D. Colombant and G. F. Tonon, "X-ray emission in laser-produced plasmas," J. Appl. Phys. **44**, 3524–3537 (1973).
9. W. Svendsen and G. O'Sullivan, "Statistics and characteristics of xuv transition arrays from laser-produced plasmas of the elements tin through iodine," Phys. Rev. A **50**, 3710–3718 (1994).
10. M. Al-Rabban, "Term structure of 4d-electron configurations and calculated spectrum in Sn-isonuclear sequence," J. Quant. Spectrosc. Radiat. Transfer., **97**, 278–316 (2006).
11. R.D. Bleach and D. J. Nagel, J.Appl. Phys. **49**, 3832–3841 (1978).
12. R.C. Spitzer, T.J. Orzechowski, D.W. Phillion, R.L. Kauffman, and C. Cerjan, J. Appl. Phys. **79**, 2251-253 (1996).
13. C-S Koay, "Radiation studies of the tin-doped microscopic drolet laser plasma light source specific to EUV lithography," Ph. D. thesis University of Central Florida, 2006.
14. S. A. George, C-S. Koay, K. Takenoshita, R. Bernath, M. Al-Rabban, C. Keyser, V. Bakshi, H. Scott, and M. Richardson, "EUV spectroscopy of mass-limited Sn-doped laser micro plasmas," Proceedings of SPIE **5751**, 779–788 (2005).

#87897 - $15.00 USD Received 28 Sep 2007; revised 15 Nov 2007; accepted 17 Nov 2007; published 26 Nov 2007

15. C-S Koay, S. George, K. Takenoshita, R. Bernath, E. Fujiwara, M. Richardson, and V. Bakshi, "High conversion efficiency microscopic tin-doped droplet target laser-plasma source for EUVL," Proc. SPIE **5751**, 279-292 (2005).
16. M. Richardson, US Patent 6865, 255, Mar. 2005.
17. F. Jin and M. Richardson, "New laser plasma source for extreme-ultraviolet lithography," Appl. Opt. **34**, 5750-5760 (1995).
18. M. C. Richardson, C-S. Koay, K. Takenoshita, C. Keyser, "High conversion efficiency mass-limited Sn-based laser plasma source for EUV lithography," J. Vac. Sci. Technol. B, **22**, 785–790 (2004).
19. K. Takenoshita, C-S Koay, S. Teerawattanasook, M. Richardson, and V. Bakshi, "Debris characterization and mitigation from microscopic laser-plasma tin-doped droplet EUV sources," Proc. SPIE **5751**, 563–571 (2005).
20. http://www.laserfocusworld.com/articles/article_display.html?id=234077
21. A. Mordovanakis, K-C. Hou, Y-C. Chang, M-Y. Cheng, J. Nees, B. Hou, A. maksimchuk, G. Mourou, B. Lafontaine, and A. Galvanauskas, Opt. Lett. **31**, 17, 2517–2519 (2006).
22. K-C. Hou et al, "Multi-MW Peak Power Scaling of Single-Transverse Mode Pulses using 80-m Core Yb-doped LMA Fibers", presented in Post Deadline Paper session at Advanced Solid-State Photonics (Optical Society of America, 2006).
23. P. Dunne, G. O'Sullivan, and D. O'Reilly, "Prepulse-enhanced narrow bandwidth soft x-ray emission from a low debris, subnanosecond, laser plasma source," Appl. Phys. Lett. **76**, 34–36 (2000).
24. S. Dusterer, H. Schwoerer, W. Ziegler, C. Ziener, and R. Sauerbrey, "Optimization of EUV radiation yield from laser-produced plasma," App. Phys. B, **73**, 693–698 (2001).
25. T. Harada and T. Kita, "Mechanically ruled aberration-corrected concave gratings," Appl. Opt. **19**, 3987–3993 (1980).
26. R. Stuik, F. Scholzeb, J.Tummler, F. Bijkerk, "Absolute calibration of a multilayer-based XUV diagnostic," Nucl. Instrum. and Methods. Phys. B **492**, 305–316 (2002).

1. Introduction

Novel lithographic techniques are needed to extend the life of current silicon microprocessors for creating smaller, powerful chips with greater number of transistors embedded. For printing structures below 22 nm, extreme ultraviolet lithography (EUVL) is being developed as the most promising alternative to deep ultraviolet lithography [1]. The EUV wavelengths are attenuated in atmosphere and are absorbed by materials. Therefore, EUVL stepper architecture will utilize reflective Mo-Si multilayer mirrors (MLM) [2] in near vacuum. The highest reflectivity in the EUV region is found for the Mo-Si MLMs with the wavelength band centered at 13.5 nm. Thus, the illumination wavelength for EUVL is chosen to be 13.5 nm.

EUVL is expected for high volume production by 2011 [3]. However, many technical challenges still remain. Vital to the success of EUVL is the availability of a technically and economically viable high repetition-rate EUV light source having sufficient brightness. Some of the critical requirements that an EUV light source needs to meet are jointly specified by the scanner developers. These are listed in table 1 [4].

Table 1. Joint requirements for EUV sources [4]

Source Characteristics	Requirements
Wavelength (nm)	13.5
EUV power at Intermediate Focus (inband) (W)	115-180
Repetition Rate (kHz)	7-10 (no upper limit
Etendue of source output (mm^2 Sr)	3.3 (design dependent)
Source Cleanliness(light-on hours)	$>$ 30,000
Spectral Purity:	
130-400 nm (%) (DUV/UV)	$<$ 3-7 (design dependent)
$>$ 400 nm	To be determined (design dependent)

The ideal source is required to have stable, high power light emission into the narrow 0.2 nm bandwidth of the multilayer optics. The etendue of the source output sets an upper limit on

#87897 - $15.00 USD Received 28 Sep 2007; revised 15 Nov 2007; accepted 17 Nov 2007; published 26 Nov 2007

the source size that can be accepted by an EUVL scanner for the maximum collectable power. Long lifetimes (>30,000 hrs) and spectral purity is also specified for an EUVL source. Source cleanliness (lifetime) is related to the length of time the multilayers can withstand continuous and high repetition rate source operation without major reflectivity degradation requiring cleaning or replacement. Absorbed off-band radiation may result in photon assisted oxidation and chemical shifts of the mirror structures. Mo-Si multilayer structures are also highly reflective in the VUV/Vis/IR region. Both of these properties make source spectral purity a requirement[3].

Existing EUV source archetypes include synchrotron radiation, high-harmonic generation from femtosecond laser pulses, discharge plasmas, and laser plasmas. The last two are considered to be the only source configurations that are capable of meeting the lithography requirements. Discharge plasma sources are efficient with electrical energy directly converted to EUV; but the electrode lifetime and the achievable output power are limited. Currently, laser generated plasmas are the most promising in the development of a practical EUV source that is capable of meeting all the necessary requirements [3]. Conversion efficiency (CE) of a laser plasma is defined as the ratio of the inband EUV power measured to the laser input power at target. Laser plasmas have demonstrated high conversion efficiencies with steadily increasing power levels [6, 7].

Focused laser radiation of intensities greater than 10^{10} W/cm^2 can ionize materials to create plasmas of high electron/ion temperature and density. Plasma temperatures can range from few electron volts (eV) to 10's of eV's depending on the laser beam parameters. The electron densities are greater than 10^{17} /cm^3. The atomic processes in hot plasmas are numerous and complex, however, the wavelengths of radiation emitted by plasmas largely depend on the average charge state population in plasmas. Ionization and recombination processes dominate the average charge state distributions which is inherently dependant on electron temperature and density [8]. EUV wavelengths can be generated and optimized for a variety of laser-target combinations by controlling the plasma temperature and density gradients.

This paper demonstrates the experimental methods employed for improving narrow-band EUV source power levels by creating electron temperature and ion density conditions that are optimum for 13.5 nm emission from fiber laser and tin-doped droplet target. Tin as a target material is advantageous since it is shown to have many transitions arising from Sn^{7+}-Sn^{13+} [9]. The ground configuration [Kr] $4p^6 4d^n$, n = 2, 3, , 7, [10] of these ions contributes to the strong unresolved transition arrays (UTA) observed in the required 2% bandwidth at 13.5nm [11, 12, 13, 14, 15]. The EUV source being developed at the Laser Plasma Laboratory (LPL) is a laser driven plasma generated from tin-doped droplets that are approximately 35 μm in diameter.

The patented source design (US patent 6,862,339) [16] utilizes mass-limited droplets [17] of tin with just enough tin atoms for the required emission [18]. Other key features of this design are the high-repetition rate droplet generation (up to 200 kHz) that can be stably synchronized to the laser pulse generation. Complete ionization of each droplet can be achieved at the end of each laser pulse with this source configuration. Full ionization and the small size of the droplet target minimizes the debris (aerosols, particles, clusters) produced during plasma generation. The source size is well within the specified etendue limits of 3.3 mm^{2}Sr [3] and debris mitigation schemes can be implemented with relative ease as needed [19]. High EUV conversion efficiencies (CE) measured for 1 Hz laser experiments were measured and reported previously [15].

2. Fiber laser system

Currently the field of fiber lasers are under rapid development. Higher powers, new wavelengths, heat dissipation characteristics, and new fibre designs for pulsed and CW applications,

#87897 - $15.00 USD Received 28 Sep 2007; revised 15 Nov 2007; accepted 17 Nov 2007; published 26 Nov 2007

poses this class of lasers as a low cost and compact alternative to solid state and gas laser technology. Kilowatt levels of power have already been demonstrated [20]. The fiber laser system used for the studies to be described here is under development at the University of Michigan, at the Center for Ultrafast Optical Sciences. At the front end of the laser is an electric-pulse-driven Fabry-Perot semiconductor laser diode emitting 1064 nm, with which repetition rate, pulse duration and pulse shape can easily manipulated. The entire system is packaged into a cascaded four-stage Master Oscillator Power Amplifier (MOPA) configuration using ytterbium-doped fiber amplifier for the seed pulse amplification to high peak powers. The beam quality of the large effective mode area (2749 μm^2) fiber is improved through coiling and mode matching techniques. The best measured beam quality factor, M^2, is 1.3 [22] to date which provides a nearly perfect gaussian beam for applications. More than 100W of power is possible from this laser, with pulse duration near 5 ns, and 5 mJ of energy per pulse. The capability of this laser system to generate pre-pulses of varying durations and delays with ease is an advantage, since prepulse [23, 24] plasmas are reported to improve the efficiency of laser energy to EUV light conversion. EUV generation from solid tin targets utilizing this laser system was demonstrated previously [21]. This study reports the first results of efficient EUV generation obtained by coupling this laser to high repetition rate source operation.

3. Experimental configuration

The vacuum chamber used for these experiments is 45 cms in diameter, with 12 vacuum ports positioned around the chamber at 30 $^\circ$ angle separation. The plasma and EUV diagnostics are set-up on the various ports of the chamber as needed. For this study, the target is positioned at the center of the chamber and the laser beam is focused with a 60 mm focal length lens mounted inside the chamber. The droplets are situated at the focus of the lens, and the laser beam is normally incident on the droplets (Fig. 1). The flat-field spectrometer (FFS) and the narrow band EUV energy detector is placed at 30 $^\circ$ on both sides of the laser beam axis (Fig. 1). Droplet generation at a rate of 31 kHz is used for these experiments and the laser pulse is synchronized to the droplet train. EUV wavelengths are generated under operating pressures better than 10^{-3} Torr.

The flat-field spectrometer [25] is used to record spectra from the source. It covers the spectral region from 11 nm-19 nm. A gold coated, variably spaced concave grating with 1200 lines/mm and a radius of curvature of 5.649 m is used in this spectrometer. The groove spacing varies from 690 nm to 990 nm. The plasma source is collimated onto the grating by an entrance slit. The design is such that the distance from the slit to the grating center is 237 mm and the distance from the grating center to the image plane is 235 mm. An X-ray charge-coupled device (CCD) camera (PI-SX, Roper Scientific) is used to record spectral images. For such a spectrometer, the slit separation determines the working spectral resolution and the slit width used is 80 μm. More details on the spectrometer design is reported previously [15, 14, 13].

The narrow bandwidth EUV emission at 13.5 nm from the source is measured with an EUV energy detector developed at the FOM-Institute for Plasma Physics Rijnhuizen [26]. This instrument consists of curved normal incidence Mo-Si MLM of known reflectivity, 0.5 μm Zr filter and an AXUV-100G photodiode. The multilayer mirror is used to select the wavelength band at approximately 3% of 13.5 nm and the Zr filter selects EUV. Measured transmission of the Zr filter in the wavelength region of interest in used in calculation. The photodiode enables time resolved, high repetition rate measurements with a spectral responsivity of 0.24 A/W at 13.5nm. The mirror used in the EUV energy detector during the experiments was sent to the National Institute of Standards and Technology (NIST) after the completion of all experiments using fiber laser.

New reflectivity data provided by NIST is used in the EUV energy calculations. The methods

#87897 - $15.00 USD Received 28 Sep 2007; revised 15 Nov 2007; accepted 17 Nov 2007; published 26 Nov 2007

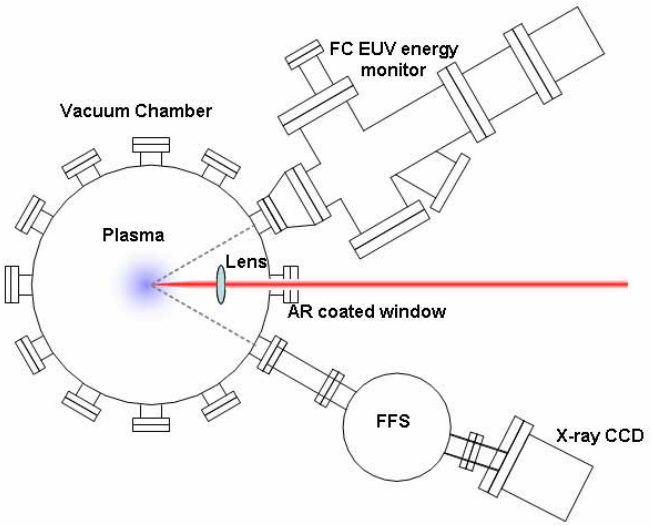

Fig. 1. Chamber set-up and diagnsotics

for calculating inband EUV energy and the CE into 2πSr and 2% BW of MLM is described in detail in previously published works [15, 13]. The spectrometer measurements are also cross-calibrated to the EUV detector, making the flat-field spectrometer a calibrated instrument for inband EUV energy measurements.

4. Results

A number of laser irradiation conditions were investigated using precision spectroscopy and calibrated metrology. Optimum conditions for generating 13.5 nm emission from the fiber laser and the tin-doped droplets are isolated. Each spectral result presented in this paper is an average of approximately 1700 shots. The CCD accumulation duration is set to 1 second. Shorter accumulation times caused blurring and smearing of the spectral information requiring additional image processing. Non-linear pixel to wavelength calibrations with respect to the prominent oxygen lines appearing in the spectral measurements were completed. The best spectral and CE results obtained with the pre-pulse plasma scale-length optimization is shown in Fig. 2.

The spectral measurements show the characteristic tin unresolved transition array centered between 13 nm and 15 nm. The four dominant oxygen lines from O^{5+} emission at 11.6, 12.98, 15.0, and 17.3 nm is observed as well. Variations in the tin unresolved transition array is seen as the intensity is varied by changing laser beam focal diameter at target. This was observed in previous experiments and was reported [15, 14]. In fig. 2(a), rapid changes in the plasma temperature is observed with the change in intensity. Figure 2(b) shows variations in the spectral counts for multiple measurements obtained at the same coupling condition. This is thought to be due to minor changes in the laser-droplet synchronization which can be improved with a target stabilization system. A target stabilization system was not in place for this study. Figure 2(c) shows that at the smallest focus (near 20 μm), the measured efficiency is lower. Figure 2(d) illustrates CE as a function of in laser beam intensity, with the best efficiency is obtained for irradiance intensities near $8 \times 10^{10}\ W/cm^2$. At the higher beam intensity with smaller focus, the calculated CE is decreased.

#87897 - $15.00 USD Received 28 Sep 2007; revised 15 Nov 2007; accepted 17 Nov 2007; published 26 Nov 2007

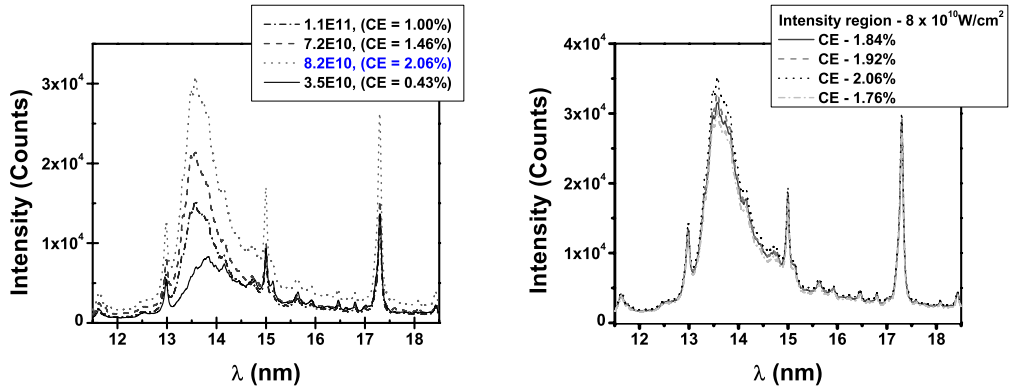

(a) Spectra as a function of intensity for varying laser beam spot size obtained by translating the focusing lens

(b) Multiple measurements taken at the best CE condition

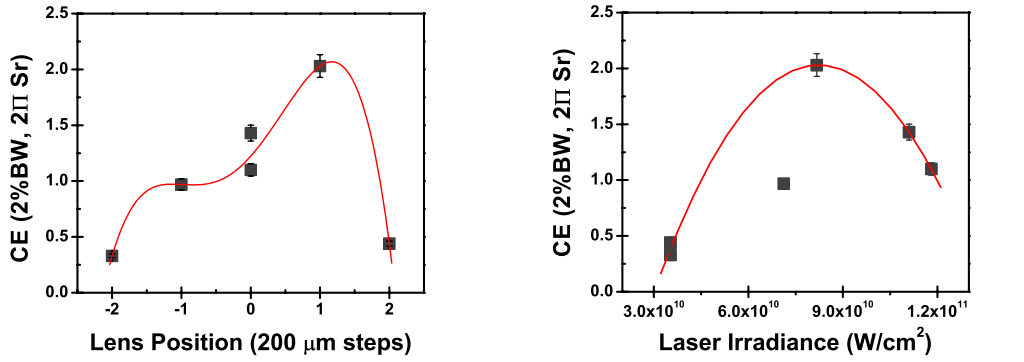

(c) Conversion efficiency into 2π Sr/2%BW as a function of lens position

(d) Conversion efficiency into 2π Sr/2%BW as a function of intensity

Fig. 2. Best results obtained for 13.5 nm generation from tin-doped droplets using the fiber laser.

The CE measurements were obtained with the laser running at 10 W. This laser power is measured before the faraday isolator that is in place to remove feedback from plasma/target to the output fiber. The isolator is installed prior to the optics directing the beam to the chamber. At the start of the experiment, the laser energy recorded at target is 80 % of the laser energy measured before the isolator. The laser energy in the chamber is also measured after the experiment to check for transmission loss of the focusing lens. The total transmission in chamber through the isolator, mirrors, window and the lens is 51.4% for the set of experiments reported in this paper. This drop in the total energy transmission is taken into account in the CE measurements.

The highest conversion efficiencies measured are found to be near irradiances of 8×10^{10} W/cm^2. The energy per pulse used in this case is 6 mJ and the pulse duration is 6.0 ns. The best CE measurement yields an efficiency of 2.1 % into 2π Sr/2%BW. To check the repeatability of the results, multiple measurements were taken at each experimental condition. The averaged CE then is approximately 1.9 %.

#87897 - $15.00 USD Received 28 Sep 2007; revised 15 Nov 2007; accepted 17 Nov 2007; published 26 Nov 2007

To compare how the generation of pre-plasma affects the EUV generation, a set of measurements without pre-pulse heating of the target was obtained. The results from these energy measurements are shown in Fig. 3. In Fig. 3(a) the best results obtained are shown with the high CE of 1% measured at the focus of the lens. Obviously, this CE measurement is only half of the highest conversion efficiency obtained for the previous set of measurements. It is interesting to note that the same CE value (1.0 %)) is found at the focal region in 2c). Figure 3(b) shows linear increase on CE with increasing laser irradiance.

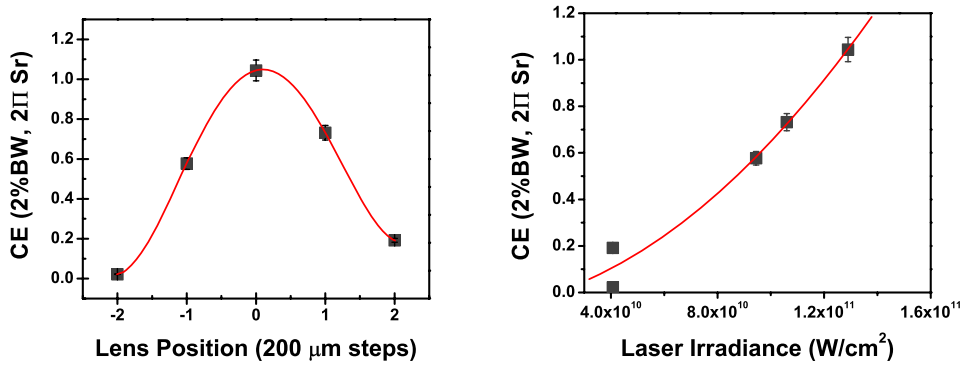

(a) Conversion efficiency into 2π Sr/2%BW as a function of lens focus

(b) Conversion efficiency into 2π Sr/2%BW as a function of the laser beam intensity

Fig. 3. Energy measurements obtained without the generation of pre-plasma for scale-length optimization. Energies measured are much lower.

Another unique characteristic of the fiber laser used here is its capability for changing pulse width as needed. For comparison to the previous results, the best result obtained from short pulse duration is plotted together and this is shown in Fig. 4. Figure 4(a) shows the true spectral results and fig. 4(b) gives the same spectra normalized to the 12.98 nm oxygen peak. Even though the irradiance intensity is much higher for the short pulse measurement, it does not translate into high average plasma electron temperature. Thus, we do not see the emission levels expected from the target. An explanation for this may be that short laser pulses result in short laser-plasma interaction lengths. Further investigation is necessary for conclusive results in this area.

In all of the previous results, for attaining the higher intensities, a short focal length lens was used which provided smaller beam focus. In all of the experiments, large tin particulate deposits on the focussing lens was observed. This lead to rapid transmission loss during experiments that is difficult to account for in the CE calculations. Figure 5 is the surface of the lens obtained using a scanning white light interferometer. The focal spot obtained with the short focal length lens is considerably smaller than the diameter of the droplet. An explanation for this is that his condition, where there is a smaller spot with low laser energy near 3-5 mJ, fails to ionize the target fully, leading excess deposits on optics. It was found that cleaning the lens surface immediately after the experiments preserved the antireflection coating on the lens. Eventually the coating was etched to a point that there were noticeable focal distortions, rendering it unviable for further use. In our previous experiments with laser pulse energies of 100 mJ and a droplet diameter of 35μm, debris is minimized [19].

#87897 - $15.00 USD Received 28 Sep 2007; revised 15 Nov 2007; accepted 17 Nov 2007; published 26 Nov 2007

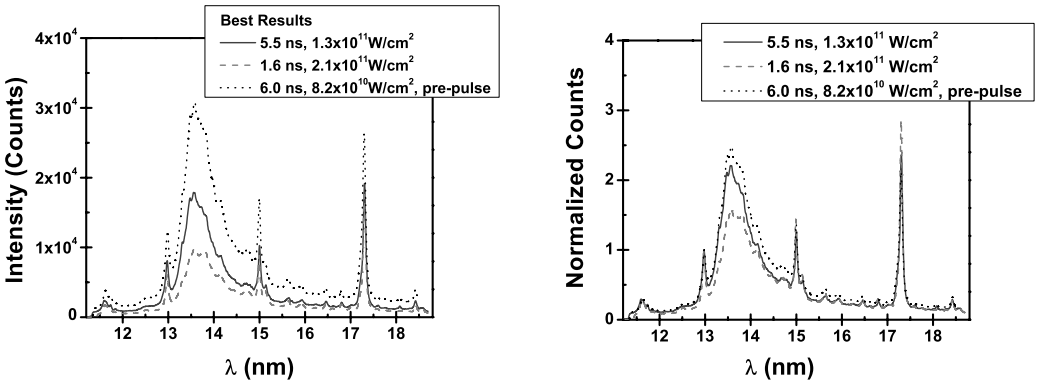

(a) Highest spectral results obtained for different laser pulse widths

(b) Normalized with 13 nm oxygen line

Fig. 4. Comparing the effect of pulse duration on plasma temperature

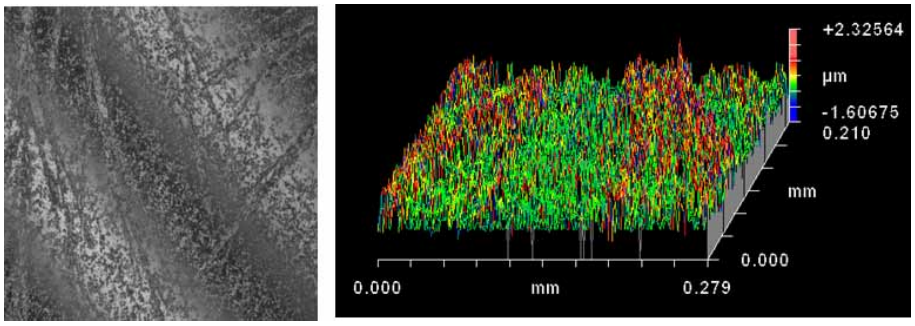

Fig. 5. Particulate deposited on the lens during an experiment with tin droplets

5. Discussion

To produce efficient EUV emission from a source material, it is necessary to ensure conditions for maximum laser energy absorption. Not only that, almost all of the absorbed laser energy needs to be converted into thermal energy capable of producing the required excited states for emission into a given wavelength region. One way to maximize laser absorption is to keep laser irradiance intensities below threshold conditions for creating parametric instabilities in the plasma.

With the tin-doped droplets and fiber laser, this experimental study demonstrates two results that will impact the EUV source development. First, it can be seen that efficient, high-power, and high repetition rate source operation is possible with fiber lasers. Second, high CE for 13.5 nm can be obtained with low laser energy per pulse as long the plasma scale length is optimized for the required emission. Figure 6 compares the best spectral measurement obtained with the 1 Hz laser at 100 mJ and 35 μm beam diameter to one of the best spectrum generated with the fiber laser. Both spectra are normalized to the oxygen peak at 12.98 nm. The wavelength scale in the solid-state laser generated spectral measurement is slightly offset to better illustrate the differences in the spectra.

#87897 - $15.00 USD Received 28 Sep 2007; revised 15 Nov 2007; accepted 17 Nov 2007; published 26 Nov 2007

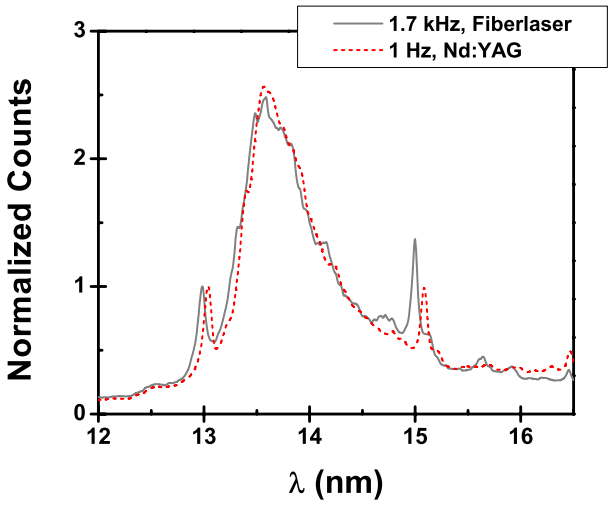

Fig. 6. Comparison of fiber laser spectral measurement to the highest Nd:YAG laser measurement for the same target

The target conditions are identical and it can be seen from Fig. 6 that the fiber laser has successfully emulated solid-state laser results, and gives identical CE results near 2.0 %. Higher conversion efficiency from the fiber laser is expected with the installation of the target stabilization system and smaller droplets. Matching the droplet diameter to the laser beam diameter at focus may reduce the debris produced during plasma generation.

Acknowledgements

The funding for this study was provided by SRC, Cymer, AMD, and the state of Florida. The authors greatly appreciate the technical assistance and discussions with Robert Bernath, Jiyeon Choi, Tobias Schmid, Jose Cunado, and Dr. Bruno LaFontaine at AMD. We would like to thank Dr. Steven Grantham for providing calibrations of the multilayer mirrors being used for the experiments.

#87897 - $15.00 USD Received 28 Sep 2007; revised 15 Nov 2007; accepted 17 Nov 2007; published 26 Nov 2007